Eur. Phys. J. A (2024) 60:60
https://doi.org/10.1140/epja/s10050-024-01275-w

THE EUROPEAN PHYSICAL JOURNAL A

Regular Article - Experimental Physics

Cross-section of the ^{95}Nb production on natural molybdenum at the bremsstrahlung end-point energy up to 95 MeV

I. S. Timchenko[1,2,a], **O. S. Deiev**[2], **S. M. Olejnik**[2], **S. M. Potin**[2], **V. A. Kushnir**[2], **V. V. Mytrochenko**[2], **S. A. Perezhogin**[2]

[1] Institute of Physics, Slovak Academy of Sciences, 84511 Bratislava, Slovakia
[2] National Science Center "Kharkov Institute of Physics and Technology", 1, Akademichna St., 61108 Kharkiv, Ukraine

Received: 6 November 2023 / Accepted: 19 February 2024 / Published online: 12 March 2024

Communicated by Navin Alahari

Abstract The photoproduction of ^{95m}Nb on ^{nat}Mo was studied using the electron beam of the LUE-40 linac RDC "Accelerator" NSC KIPT. Measurements were performed using activation and off-line γ-ray spectrometric techniques. The experimental flux-averaged cross-section $\langle\sigma(E_{\gamma max})\rangle_m$ for the ^{nat}Mo$(\gamma, xnp)^{95m}$Nb reaction at the bremsstrahlung end-point energy range of 38–93 MeV has been first time obtained. The estimated values $\langle\sigma(E_{\gamma max})\rangle_g$ for the formation of ^{95}Nb in the ground state and total cross-sections $\langle\sigma(E_{\gamma max})\rangle_{tot}$ for the studied reaction were determined. The theoretical values of the yields $Y_{m,g,tot}(E_{\gamma max})$ and flux-averaged cross-sections $\langle\sigma(E_{\gamma max})\rangle_{m,g,tot}$ for the ^{nat}Mo$(\gamma, xnp)^{95m,g,tot}$Nb reactions were calculated using the cross-sections $\sigma(E)$ from the TALYS1.95 code for six different level density models. The comparison showed a significant excess of the experimental results over the theoretical $\langle\sigma(E_{\gamma max})\rangle_{m,g,tot}$ values.

1 Introduction

Experimental data on cross-sections for photonuclear reactions are important for many fields of science and technology. These data are necessary for traditional studies of the Giant Dipole Resonance (GDR), and mechanisms of its excitation and decay including competition between statistical and direct processes in decay channels, GDR configurational and isospin splitting, sum rule exhaustion, etc. The cross-sections for photonuclear reactions are also widely used in various applications, primarily in astrophysics [1], medicine [2], design of fast reactors [3] and accelerator driven subcritical systems [4,5].

There is a problem of discrepancy between experimental data on cross-sections (γ, n), $(\gamma, 2n)$, $(\gamma, 3n)$, measured in different laboratories [6–14]. The development of modern theoretical models to describe the mechanisms of nuclear reactions and program codes [15–18] based on these concepts requires verification using data on multiparticle photonuclear reactions (γ, xn) and $(\gamma, xnyp)$. In addition, there is a lack of such data in international databases [19–23]. This led to works on the analysis of the reliability of previously measured experimental cross-sections [24], and initiated new measurements, e.g. [25–30].

A particularly difficult case is photonuclear reactions with the emission of charged particles. The cross-sections of such reactions are usually very small for nuclei of medium and heavy masses, and there are significant discrepancies between the experimental results and the calculation of cross-sections for photonuclear reactions in the TALYS code for example, see [31,32]. In the case of light nuclei, a divergence of cross-sections is also observed, for example, [33].

In the case of photoproton reactions, an analysis is also required to establish patterns and criteria for data reliability, as, for example, shown in [34]. However, there is a lack of experimental data, especially in the region of nuclei with a mass number $A > 100$ for which the (γ, p) reaction yields are strongly suppressed.

Multiparticle photonuclear reactions have small cross-sections that can be measured using intense fluxes of incident γ-quanta [30–33]. Such γ-quanta fluxes can be produced by linear electron accelerators using a converter to generate bremsstrahlung radiation. This type of experiment allows measuring integral characteristics of reactions, such as reaction yield [35,36], flux-average cross-section [37–40], cross-section per equivalent photon [41–43], etc., and requires additional mathematical processing of the results.

[a] e-mails: iryna.timchenko@savba.sk; timchenko@kipt.kharkov.ua (corresponding author)

Despite this, bremsstrahlung remains an important tool in the study of photonuclear reactions.

Experiments on the photodisintegration of stable isotopes of the Mo nucleus were described in literature, for example, [32,35,36,41,44–52]. However, the photodisintegration of the Mo nucleus with the formation of ^{95}Nb has not been studied much. The values of the isomer ratio for the ^{95m,g}Nb nuclei-product in reactions on natural molybdenum were mainly obtained [44–48]. The data obtained in the region of GDR have been presented in different ways and some of them contradict each other [47,48].

At an intermediate energy region for the isomer ratios for the ^{nat}Mo(γ, $x$np)^{95m,g}Nb reaction were measured in Ref. [32,35,36,49,50]. All these data are in good agreement with each other, but show a marked difference from the theoretical predictions based on cross-sections $\sigma(E)$ from the TALYS1.95 code for six different level density models (see Ref. [32]). For a more detailed analysis of theoretical models, it is necessary to compare theoretical estimates with experimental cross-sections of the ^{nat}Mo(γ, $x$np)^{95m,g}Nb reactions.

There is little data in the literature on a cross-section of the reaction ^{nat}Mo(γ, $x$np)^{95m}Nb. The activation yield curves have been presented in [41] for a number of photonuclear reactions in the energy range from 30 to 68 MeV, in order to evaluate quantitatively the interferences due to competing reactions in multielement photon activation analysis. As a result, in [41] the energy dependence of the yield of the ^{96}Mo(γ, $x$np)^{95m}Nb reaction was obtained in the terms of the average cross-section per equivalent photon.

In this work a study of the ^{95m,g}Nb production in photonuclear reactions on ^{nat}Mo at the bremsstrahlung end-point energy range of $E_{\gamma max}$ = 38–93 MeV is performed. The obtained experimental results are compared with data from Ref. [41] and theoretical estimates performed with the cross-sections $\sigma(E)$ from the TALYS1.95 code with different level density models LD 1–6.

2 Experimental setup and procedure

The experimental measuring complex of our laboratory for the study of photonuclear reactions and in particular for the study of the formation of the ^{95m}Nb nucleus in reactions on ^{nat}Mo is shown in the form of a block diagram in Fig. 1.

The experiment was performed using the electron linear accelerator LUE-40 of Research and Development Center "Accelerator" of the National Science Center "Kharkov Institute of Physics and Technology" at the range of initial electron energy is E_e = 30–100 MeV. Previously, we described in detail the parameters of the linear accelerator LUE-40, which can be found in [53–56]. Description of the details of the experiment (irradiation of targets, measurement of spectra of γ-induced activity, modeling of the bremsstrahlung fluxes using the GEANT4.9.2 code [57], and procedure of monitoring the bremsstrahlung flux with the yield of the ^{100}Mo(γ, n)^{99}Mo reaction) can be found in papers [30,37,58–60].

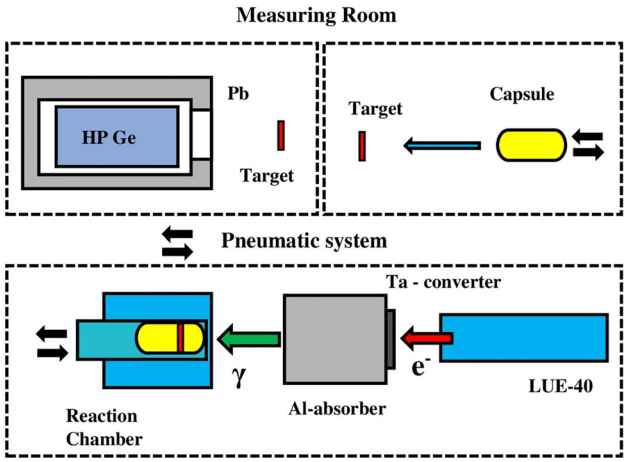

Fig. 1 Block diagram of the experiment. The lower part shows the linear accelerator LUE-40, the Ta converter, the Al absorber, and the exposure reaction chamber. The upper part shows the measuring room

The irradiated Ta converter and Al absorber generate neutrons that can trigger the reaction ^{100}Mo(n, 2n)^{99}Mo. To evaluate also this option, energy spectra of neutrons above the threshold energies and neutron cross-sections were calculated using the GEANT4.9.2 and TALYS1.95. The contribution of the ^{100}Mo(n, 2n)^{99}Mo reaction to the value of the induced activity of the ^{99}Mo nucleus has been estimated and it has been shown that this contribution is negligible compared to the contribution of ^{100}Mo(γ, n)^{99}Mo.

For the experiment the targets were made of natural molybdenum. The shape of the targets were thin foil discs with a diameter of 8 mm and a thickness of ≈ 0.11 mm, which corresponds to a mass of ≈60 mg. Natural molybdenum consists of 7 stable isotopes, with isotopic abundances: ^{92}Mo – 0.1484, ^{94}Mo – 0.0925, ^{95}Mo – 0.1592, ^{96}Mo – 0.1668, ^{97}Mo – 0.0955, ^{98}Mo – 0.2413, ^{100}Mo – 0.0963 (according [16,57]).

The measurements of the induced γ-activity of the irradiated targets were performed using a Canberra HPGe detector with a full width half maximum resolution 0.8 and 1.8 keV for the energies E_γ = 122 and 1332 keV, respectively, and an efficiency of 20%, relative to the NaI(Tl)-detector with dimensions 3 inches in diameter and 3 inches in thickness. The HPGe detector was placed in a special lead tube, which significantly improved the background measurement conditions. To calibrate the spectrometric channel in terms of energy E_γ and absolute efficiency of registration of γ-quanta, reference sources of γ-radiation ^{22}Na, ^{60}Co, ^{133}Ba, ^{137}Cs, ^{152}Eu, and ^{241}Am were used.

As an example, the γ-radiation spectrum of a ^{nat}Mo target is shown in Fig. 2. As can be seen, the γ-radiation spectrum of a natural molybdenum target is a complex pattern. There are many peaks corresponding the γ-lines from the ^{nat}Mo(γ, xnyp) reactions.

3 Calculation of cross-sections, flux-averaged cross-sections, and yields of photonuclear reactions

The photonuclear reactions ^{nat}Mo(γ, $x$np) nucleus formed metastable and ground states of ^{95m,g}Nb. Natural molybdenum consists of seven stable isotopes, but only four isotopes took part in the formation of the ^{95}Nb nucleus. Respectively, there are four reactions with different thresholds:

^{96}Mo(γ, p)^{95g}Nb – E_{thr} = 9.30 MeV;
^{97}Mo(γ, np)^{95g}Nb – E_{thr} = 16.12 MeV;
^{98}Mo(γ, 2np)^{95g}Nb – E_{thr} = 24.76 MeV;
^{100}Mo(γ, 4np)^{95g}Nb – E_{thr} = 38.98 MeV.

The thresholds for the metastable state ^{95m}Nb formation nucleus are higher than in the ground state with an additional excitation energy of 235.7 keV.

The theoretical cross-sections $\sigma(E)$ of studied reactions for monochromatic photons were calculated using the TALYS1.95 code [16] for different level density models LD 1–6. In the TALYS code, there are three phenomenological level density models and three options for microscopic level densities. Descriptions of the models are given in [16]:

$LD1$: Constant temperature + Fermi gas model, introduced by Gilbert and Cameron [61].
$LD2$: Back-shifted Fermi gas model [62].
$LD3$: Generalized superfluid model (GSM) [63,64].
$LD4$: Microscopic level densities (Skyrme force) from Goriely's tables [65].
$LD5$: Microscopic level densities (Skyrme force) from Hilaire's combinatorial tables [66].
$LD6$: Microscopic level densities based on temperature-dependent Hartree-Fock-Bogoliubov calculations using the Gogny force [67] from Hilaire's combinatorial tables.

Figure 3a–c shows the calculated cross-sections $\sigma(E)$ for the formation of the ^{95m,g,tot}Nb nucleus on 4 stable isotopes of molybdenum: ^{96}Mo, ^{97}Mo, ^{98}Mo, and ^{100}Mo. These cross-sections take into account the percentage abundance of isotopes. In all three cases, the cross-sections for natural molybdenum (black curve) were obtained as the sum of the cross-sections for 4 isotopes with the percentage abundance of isotopes.

As can be seen from Fig. 3a, at an energy range of the GDR, the main contribution to the formation of the nucleus ^{95m}Nb is given by the ^{96}Mo(γ, p) reaction. For energy above 30 MeV, all other isotopes need to be taken into account for the formation of the ^{95m}Nb. In the energy dependence of the cross-section of the ^{95m}Nb nucleus formation, the dominance of a contribution of the ^{96}Mo isotope is noticeable, while for ^{95g}Nb the contribution of the cross-sections on the four Mo isotopes is more evenly distributed. The calculations have been performed for the TALYS1.95 code, level density model $LD1$.

Note that the results calculated for other level density models retain a similar tendency between the contributions of 4 isotopes to the cross-sections for the formation of the ^{95}Nb nucleus (dominance of a contribution of the ^{96}Mo isotope for ^{95m}Nb, and more balanced contribution for ^{95g,tot}Nb).

The calculated reaction yield, using theoretical cross-sections $\sigma(E)$, is determined by the formula:

$$Y(E_{\gamma max}) = N_n \int_{E_{thr}}^{E_{\gamma max}} \sigma(E) \cdot W(E, E_{\gamma max}) dE, \quad (1)$$

where N_n is the number of atoms of the element under study, $W(E, E_{\gamma max})$ is the bremsstrahlung γ-flux.

For the estimation of the contribution of a reaction in the total production of a studied nuclide (for example, the ^{96}Mo(γ, p) reaction in the production of the ^{95}Nb nucleus on ^{nat}Mo), the normalized reaction yield $Y_i(E_{\gamma max})$ was used. For calculation of $Y_i(E_{\gamma max})$ it was used the expression:

$$Y_i(E_{\gamma max}) = \frac{A_i \int_{E^i_{thr}}^{E_{\gamma max}} \sigma_i(E) \cdot W(E, E_{\gamma max}) dE}{\sum_{k=1}^{4} A_k \int_{E^k_{thr}}^{E_{\gamma max}} \sigma_k(E) \cdot W(E, E_{\gamma max}) dE}, \quad (2)$$

where $\sigma_k(E)$ is the cross-section for the formation of the ^{95}Nb nucleus on the k-th isotope with isotopic abundance A_k. Summation over k was carried out for 4 stable molybdenum isotopes ^{96,97,98,100}Mo.

Figure 4a–c shows the normalized yields of various isotopes of the reaction ^{nat}Mo(γ, $x$np)$^{95\,m,g,tot}$Nb according to Eq. 2. The value of the normalized yield on a given isotope is determined by the cross-section, the reaction threshold, and the isotope percentage abundance.

As a rule, in the presence of several isotopes, there is one whose contribution to the reaction yield dominates ($> 90\%$), as shown, for example, in Refs. [25,38]. In the case of the reaction ^{nat}Mo(γ, $x$np)^{95m}Nb at energies up to 20 MeV, the contribution of ^{96}Mo is 100%. With increasing energy, the contribution from isotope ^{96}Mo decreases but remains dominant over the entire energy range under study. In the case of the formation of the ^{95}Nb nucleus in the ground state at bremsstrahlung end-point energy above 30 MeV, it is difficult to determine the dominant reaction. Thus, for the

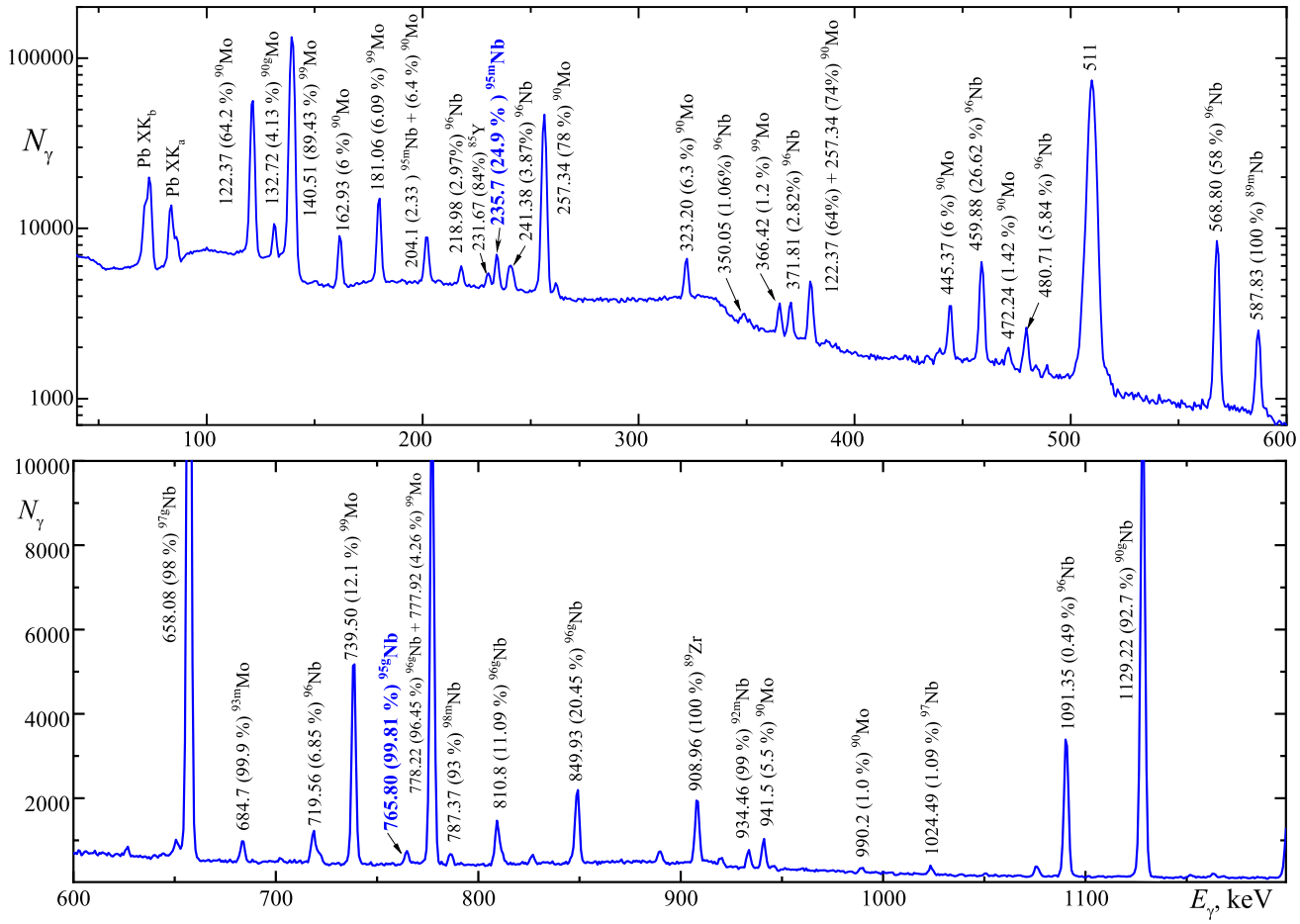

Fig. 2 Two fragments of γ-ray spectrum in the energy ranges $40 \leq E_\gamma \leq 600$ keV and $600 \leq E_\gamma \leq 1200$ keV from the ^{nat}Mo target of mass 57.862 mg after irradiation of the bremsstrahlung γ-flux at the end-point energy $E_{\gamma max} = 92.50$ MeV. The irradiation t_{irr} and measurement t_{meas} times were both 3600 s

estimation of the yield of the ^{nat}Mo$(\gamma, x$np) reaction with the production of the ^{95}Nb nucleus in the ground state it is necessary to take into account the contribution of the four stable isotopes.

The cross-sections $\sigma(E)$ for ^{nat}Mo$(\gamma, x$np$)^{95m,g,tot}$Nb reactions, calculated in TALYS1.95 for level density models LD 1–6, are shown in Fig. 5a–c.

The cross-sections $\sigma(E)$ are averaged over the bremsstrahlung flux $W(E, E_{\gamma max})$ in the energy range from the threshold of the reaction E_{thr} to the maximum energy of the bremsstrahlung spectrum $E_{\gamma max}$. As a result, flux-averaged cross-sections were obtained:

$$\langle \sigma(E_{\gamma max}) \rangle_{th} = \frac{\int_{E_{thr}}^{E_{\gamma max}} \sigma(E) \cdot W(E, E_{\gamma max}) dE}{\int_{E_{thr}}^{E_{\gamma max}} W(E, E_{\gamma max}) dE}. \quad (3)$$

For calculation of flux-averaged cross-sections $\langle \sigma(E_{\gamma max}) \rangle$ for the ^{nat}Mo$(\gamma, x$np$)^{95m,g}$Nb reactions, we average the cross-sections $\sigma(E)$ using minimal reaction thresholds: in the case formation of ^{95m}Nb – $E_{thr} = 9.54$ MeV and ^{95g}Nb – $E_{thr} = 9.30$ MeV. This was done to be able to compare the theoretical flux-averaged cross-sections with experimental results, where the total flux from the ^{96}Mo threshold to $E_{\gamma max}$ is also used. If, in making calculations, we use a self-own reaction threshold for each isotope, as we did in [25,68], then it is necessary to introduce an appropriate correction factor. Since such a coefficient is theoretically dependent, we do not use this approach in this work.

The results of the flux-averaged cross-section $\langle \sigma(E_{\gamma max}) \rangle$ calculation for the ^{nat}Mo$(\gamma, x$np$)^{95m,g,tot}$Nb reactions are presented in Fig. 6.

The shape of the energy dependence of the cross-sections for the formation of metastable and ground states is noticeably different. In the case of the metastable state, we observe the dominance of the contribution from ^{96}Mo (Fig. 5a, energies of about 20 MeV). This leads to rapid saturation of the flux-averaged cross-section for the metastable state (Fig. 6a). In the case of ground and total cross-sections, the contributions of isotope cross-sections are distributed more evenly, and the flux-averaged cross-sections increase

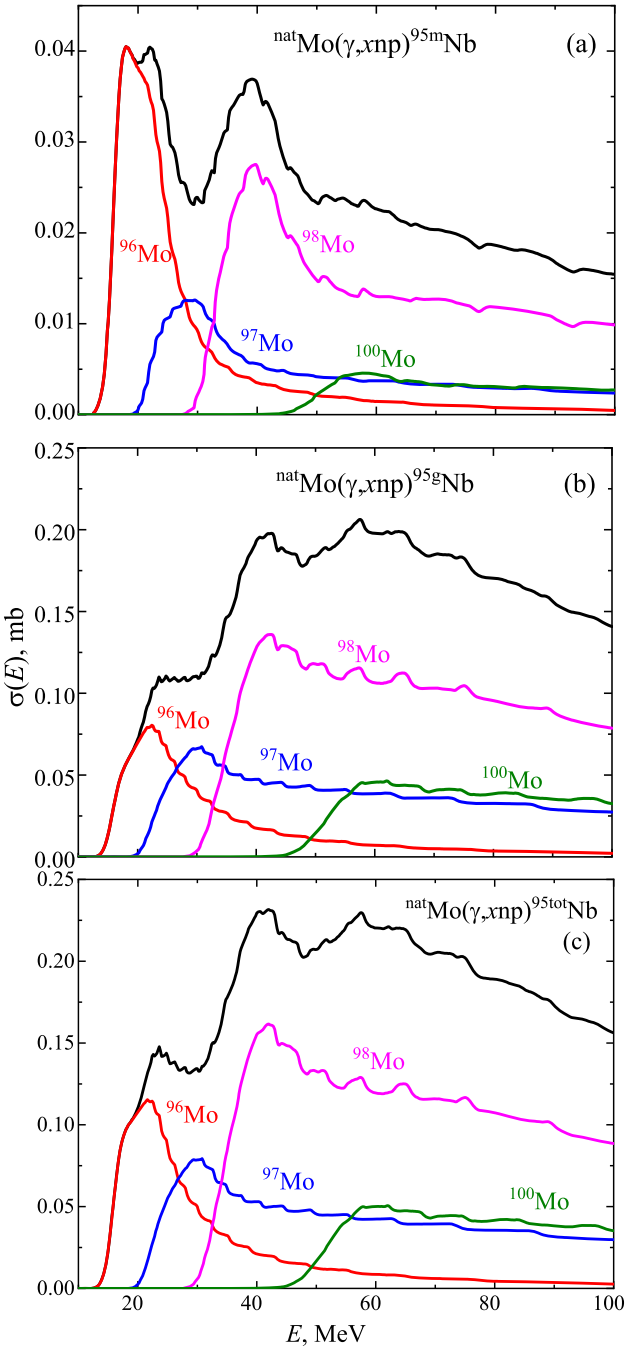

Fig. 3 Theoretical cross-sections $\sigma(E)$ for the formation of the ^{95m,g,tot}Nb nucleus on 4 stable isotopes of molybdenum (taking into account isotope percentage abundance) and on ^{nat}Mo (black curve). Results for production of the ^{95}Nb nucleus in a metastable (**a**), and ground (**b**) states, total cross-sections (**c**) are shown. The calculations were performed in the TALYS1.95 code, $LD1$

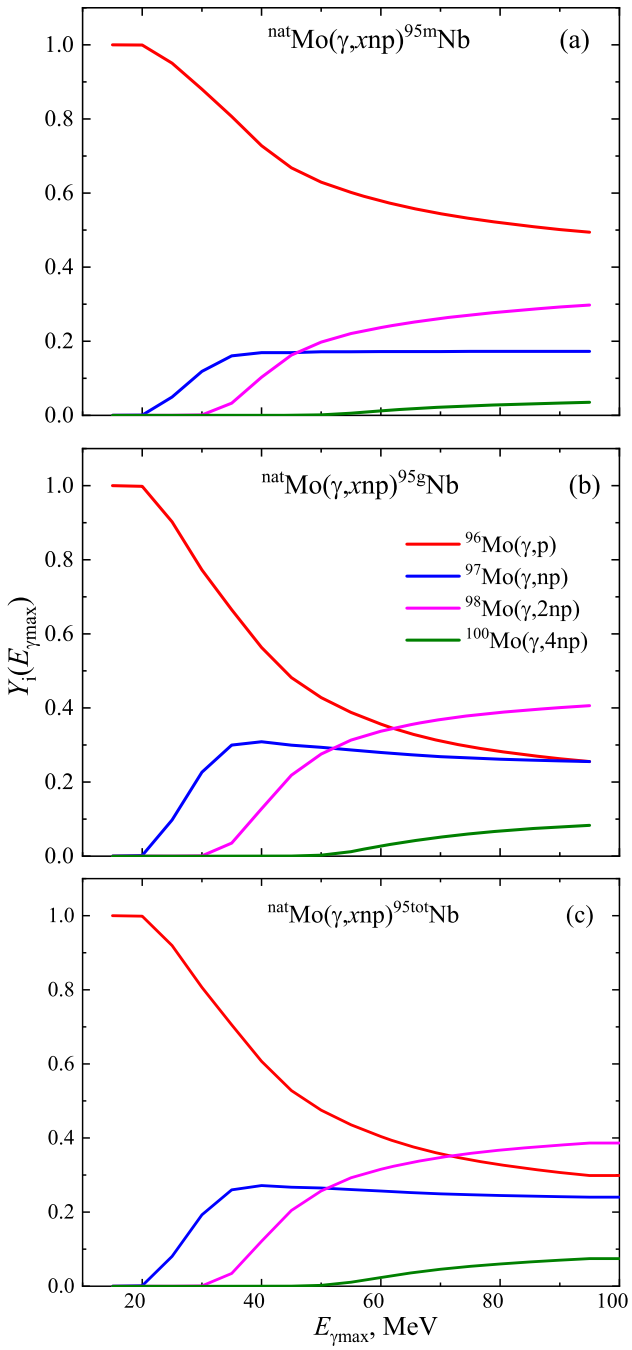

Fig. 4 The normalized reaction yields of the ^{95}Nb formation on various molybdenum isotopes. The sum of the isotope normalized yields is equal to 1. Results for the formation of the ^{95}Nb nucleus in the metastable (**a**), in the ground (**b**) states, and for total cross-section (**c**) are shown. The calculations were performed in the TALYS1.95 code, $LD1$

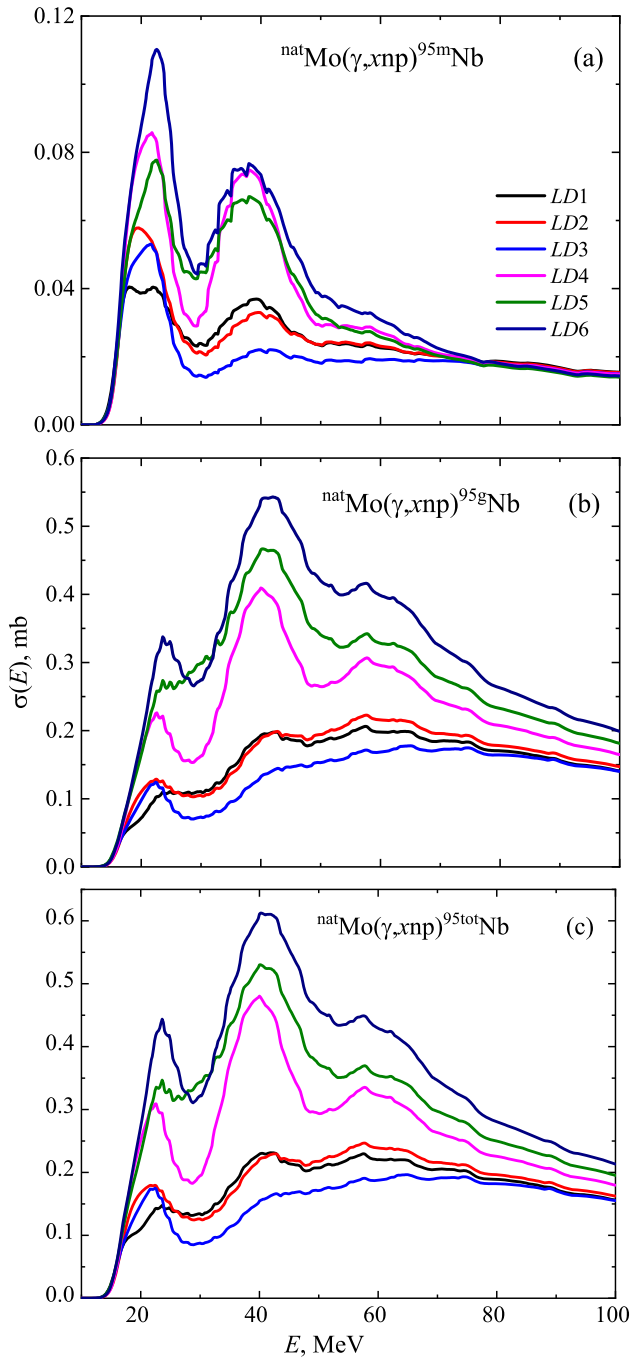

Fig. 5 Theoretical cross-sections $\sigma(E)$ for the $^{nat}Mo(\gamma, xnp)^{95m,g,tot}Nb$ reactions. The calculations were performed using the TALYS1.95 code for six different level density models

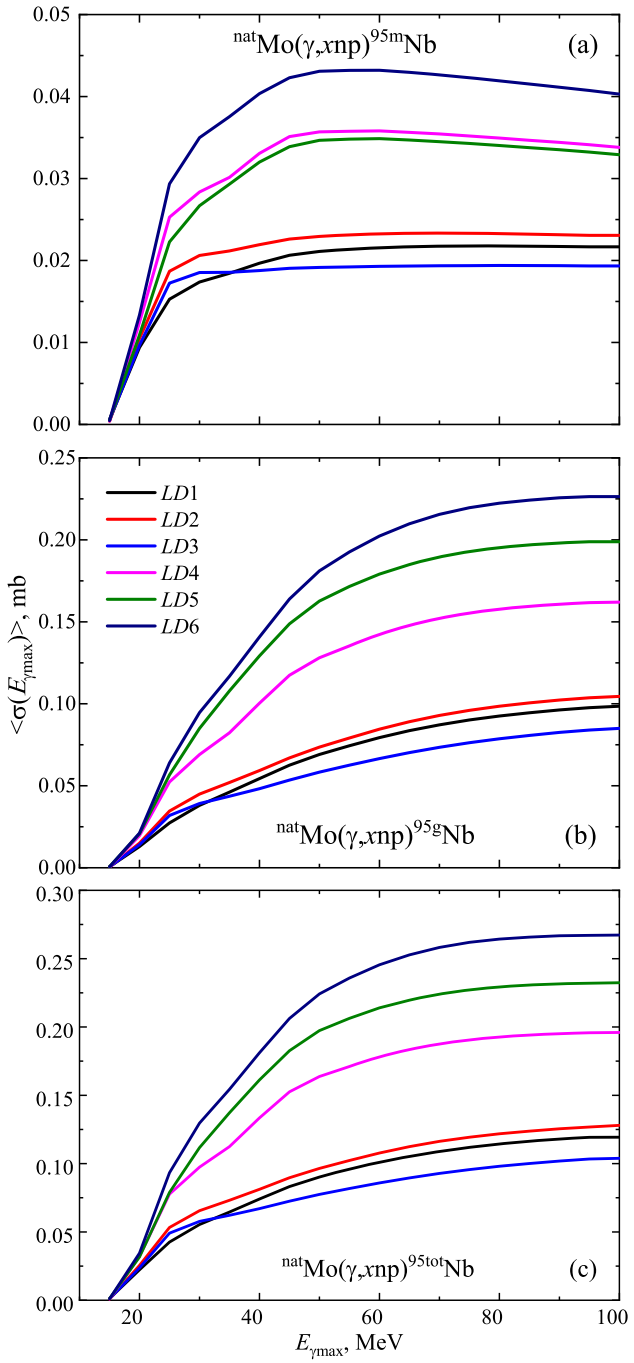

Fig. 6 Theoretical flux-averaged cross-sections $\langle\sigma(E_{\gamma max})\rangle$ for the $^{nat}Mo(\gamma, xnp)^{95m,g,tot}Nb$ reactions. The calculations were performed using the minimal reaction thresholds and the TALYS1.95 code for six different level density models

smoothly up to 95 MeV. Note that the cross-sections for the ^{96,97,98,100}Mo nuclei are given taking into account the percentage abundance of isotopes. The cross-sections of the $^{nat}Mo(\gamma, xnp)^{95tot}Nb$ reaction are their algebraic sum.

4 Experimental results

A simplified diagram of the decay of the ^{95}Nb nucleus from the ground and metastable states is shown in Fig. 7. Nuclear spectroscopic data of the radio-nuclides reactions $^{nat}Mo(\gamma, xnp)^{95m,g}Nb$ are presented according to [23].

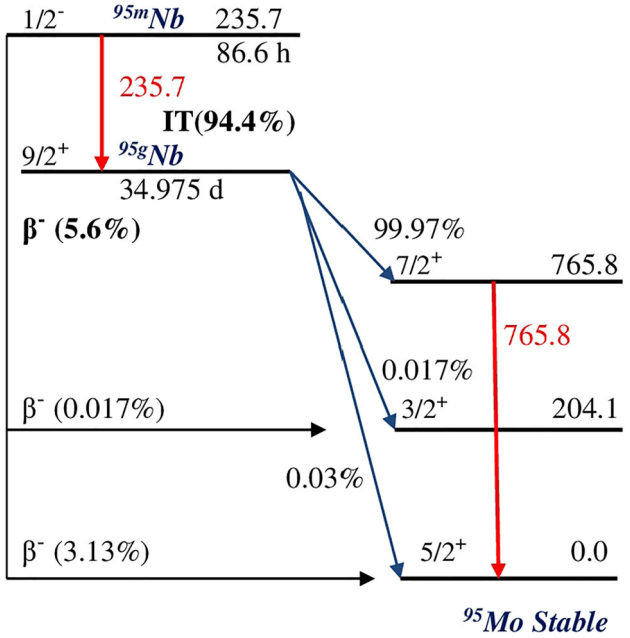

Fig. 7 Simplified representation of formation and decay scheme of the isomeric pair ^{95m,g}Nb. The nuclear level energies are in keV

The isomeric state ^{95m}Nb ($J^{\pi} = 1/2^{-}$) with a half-life $T_{1/2}$ of 86.6 ± 0.08 h decays to the unstable ground state ^{95g}Nb ($J^{\pi} = 9/2^{+}$) by emitting γ-quanta with the energy of 235.7 keV through an internal transition with a branching ratio p of 94.4 ± 0.6%. Meanwhile, 5.6% of the isomeric state decays to the various energy levels of stable ^{95}Mo via β^{-}-process. The unstable ground state ^{95g}Nb with a half-life $T_{1/2}$ of 34.975 ± 0.007 d decays to the 765.8 keV energy level of ^{95}Mo via β^{-}-process (99.97%).

The cross-sections for the formation of the ^{95m}Nb nucleus in the metastable state in the reaction on ^{nat}Mo can be determined from direct measurements of the number of counts of γ-quanta $\triangle A$ in the full absorption peak at an energy of 235.7 keV ($I_{\gamma} = 24.9 \pm 0.8\%$). To calculate the experimental values $\langle\sigma(E_{\gamma max})\rangle$ the following expression was used:

$$\langle\sigma(E_{\gamma max})\rangle = \frac{\lambda \triangle A \Phi^{-1}(E_{\gamma max})}{N_x I_{\gamma}\, \varepsilon (1 - e^{-\lambda t_{irr}}) e^{-\lambda t_{cool}} (1 - e^{-\lambda t_{meas}})}, \quad (4)$$

where $\Phi(E_{\gamma max}) = \int_{E_{thr}}^{E_{\gamma max}} W(E, E_{\gamma max}) dE$ is the brems strahlung flux in the energy range from the reaction threshold E_{thr} up to $E_{\gamma max}$; N_x is the number of studied atoms (including 4 isotopes of Mo – 96, 97, 98, and 100); I_{γ} is the intensity of the analyzed γ-quanta; ε is the absolute detection efficiency for the analyzed γ-quanta energy; λ denotes the decay constant ($\ln 2/T_{1/2}$); $T_{1/2}$ is the half-life of the nucleus; t_{irr}, t_{cool} and t_{meas} are the irradiation time, cooling time and measurement time, respectively.

In natural molybdenum targets, as a result of the ^{nat}Mo(γ, xn2p) reaction, the ^{95}Zr nucleus can also be formed. In the decay scheme of ^{95}Zr ($T_{1/2} = 65.02 \pm 0.05$ d) there is a γ-transition with the energy $E_{\gamma} = 235.7$ keV and intensity $I_{\gamma} = 0.294 \pm 0.016\%$. The decay of the ^{95}Zr nucleus can contribute to the observed value of ΔA. To take this contribution into account, calculations were performed in the TALYS1.95 code with level density model $LD1$. It was found that the estimated activity of ^{95}Zr by γ-line with 235.7 keV is negligible. The contribution of ^{95}Zr was also experimentally verified by the γ-lines corresponding to the decay of the ^{95}Zr nucleus, namely, $E_{\gamma} = 724.2$ keV ($I_{\gamma} = 44.17 \pm 0.13\%$) and $E_{\gamma} = 756.7$ keV ($I_{\gamma} = 54\%$). No such peaks were found in the measured spectra of the induced γ-activity of the targets.

For the γ-quanta with an energy of 235.7 keV and the thicknesses of the molybdenum targets used, the self-absorption coefficients were calculated using the GEANT4.9.2 code. It was found that the value of the self-absorption coefficient did not exceed 0.8%, which was taken into account when processing the experimental results.

The uncertainty of measured flux-averaged cross-sections was determined as a square root of the quadratic sum of statistical and systematic errors. The statistical error in the observed γ-activity is mainly due to statistics in the full absorption peak of the corresponding γ-ray, which varies between 1.1 to 4.2%. The measured $\triangle A$ value of the investigated γ ray depends on the detection efficiency, half-life, and the intensity. The background is generally governed by the contribution from the Compton scattering of the emitted γ rays.

Systematic errors are caused by the following uncertainties: exposure time and electron current ~0.5%, detection efficiency of γ-rays by the detector 2–3%, half-life $T_{1/2}$ of reaction products, and intensity I_{γ} of the analyzed γ-rays. The error of experimental data normalization to the yield of the monitoring reaction ^{100}Mo(γ, n)^{99}Mo was 6%. The systematic error in yield monitoring of the ^{100}Mo(γ, n)^{99}Mo reaction stems from three errors, each reaching up to 1%. These are the statistical error in the determination of the number of counts under the γ-ray peak used for normalization, the uncertainty in the isotopic composition of natural molybdenum and in the intensity I_{γ} used. This also includes the calculation error of the bremsstrahlung flux in GEANT4.9.2 (1−1.5%).

The total uncertainties of the measured flux-averaged cross-sections are given in Fig. 8 and Table 1.

The experimental values of the flux-averaged cross-section $\langle\sigma(E_{\gamma max})\rangle_m$ of the ^{nat}Mo(γ, $x$np)^{95m}Nb reaction were determined at the bremsstrahlung end-point energy of 38–93 MeV (see Fig. 8a and Table 1). When calculating $\langle\sigma(E_{\gamma max})\rangle_m$ values, we use flux of bremsstrahlung quanta with a threshold for the reaction on isotope ^{96}Mo, E_{thr} = 9.54 MeV.

As can be seen from the decay diagram of the isomeric and ground states of the ^{95}Nb nucleus (see Fig. 7), it is impossible to determine the value of the flux-averaged cross-section for the formation of the ^{95g}Nb nucleus in the ground state using direct measurements of the value $\triangle A$ in the full absorption peak at an energy of 765.8 keV. However, these values can be estimated using data on $\langle\sigma(E_{\gamma\max})\rangle_{\rm m}$ for the formation of ^{95m}Nb in a metastable state, obtained in this work, and the values of isomeric yield ratio $IR = Y_{\rm H}(E_{\gamma\max})/Y_{\rm L}(E_{\gamma\max})$, from the work [32]. The ^{95m}Nb nucleus in the metastable state has a low-spin state and in the ground state ^{95g}Nb has a high-spin state, then knowing the IR values, one can find the flux-averaged cross-section for the formation of the ^{95g}Nb nucleus $\langle\sigma(E_{\gamma\max})\rangle_{\rm g}$ from a simple relation: $\langle\sigma(E_{\gamma\max})\rangle_{\rm g} = \langle\sigma(E_{\gamma\max})\rangle_{\rm m} \cdot IR$. Similarly, one can estimate the total flux-averaged cross-section for the formation of a ^{95}Nb nucleus on natural Mo.

The values of $\langle\sigma(E_{\gamma\max})\rangle_{\rm g}$ and $\langle\sigma(E_{\gamma\max})\rangle_{\rm tot}$, obtained by recalculation using IR, are presented in Fig. 8b, c.

A comparison of experimental flux-averaged cross-section for ^{95m,g,tot}Nb shows a strong discrepancy with theoretical calculations. The closest to the experiment is the calculated result obtained using the cross-sections from the TALYS1.95 code for level density model $LD6$. The difference was 13.2 for the case of he formation the ^{95m}Nb nucleus in a metastable state. This factor was obtained by the least squares method. An equally strong discrepancy for the cross-section for the metastable state was also observed in the case of studying the reaction ^{181}Ta$(\gamma, {\rm p})^{180m}$Hf [31]. In the case of the formation of a ^{95g}Nb nucleus in the ground state and for the total cross-section, the calculation results are much closer to the experimental data. The comparison shows that the difference between theory and experiment was 2.7 and 4.5 times, respectively.

As noted earlier according to [19], a study of the reaction ^{96}Mo$(\gamma, {\rm p})^{95}$Nb was performed in [41], and experimental values of the average cross-section per equivalent photon $\langle\sigma(E_{\gamma\max})\rangle_{\rm Q}$ were obtained. For comparison with these data, we presented our experimental results as $\langle\sigma(E_{\gamma\max})\rangle_{\rm Q}$. To determine the value of the averaged cross-sections per equivalent photon, a formula was used, that written in [41] as:

$$\left\langle\sigma\left(E_{\gamma\max}\right)\right\rangle_{\rm Q} = \frac{\int_{E_{\rm thr}}^{E_{\gamma\max}} \sigma(E)\cdot W(E, E_{\gamma\max})dE}{\frac{1}{E_{\gamma\max}}\int_{E_{\rm thr}}^{E_{\gamma\max}} E\cdot W(E, E_{\gamma\max})dE}. \quad (5)$$

First, we analyzed the cross-section for the ^{100}Mo$(\gamma, {\rm n})^{99}$ Mo reaction, which is used in our experiment as a monitoring reaction. In the case of working with natural Mo targets, this reaction occurs only on one isotope of molybdenum with an atomic mass of 100. The comparison of the results presented as $\langle\sigma(E_{\gamma\max})\rangle_{\rm Q}$ with data from [41] agreed within 4.5–7.1%, which does not exceed the experimental error of our data. This makes it possible to compare cross-sections for the reaction $^{\rm nat}$Mo$(\gamma, x{\rm np})^{95\,\rm m}$Nb under study. Note that the authors of [41] did not provide experimental errors for their results.

In [41], targets made of natural molybdenum were used. The cross-sections $\langle\sigma(E_{\gamma\max})\rangle_{\rm Q}$ for the ^{96}Mo$(\gamma, {\rm p})^{95m}$Nb

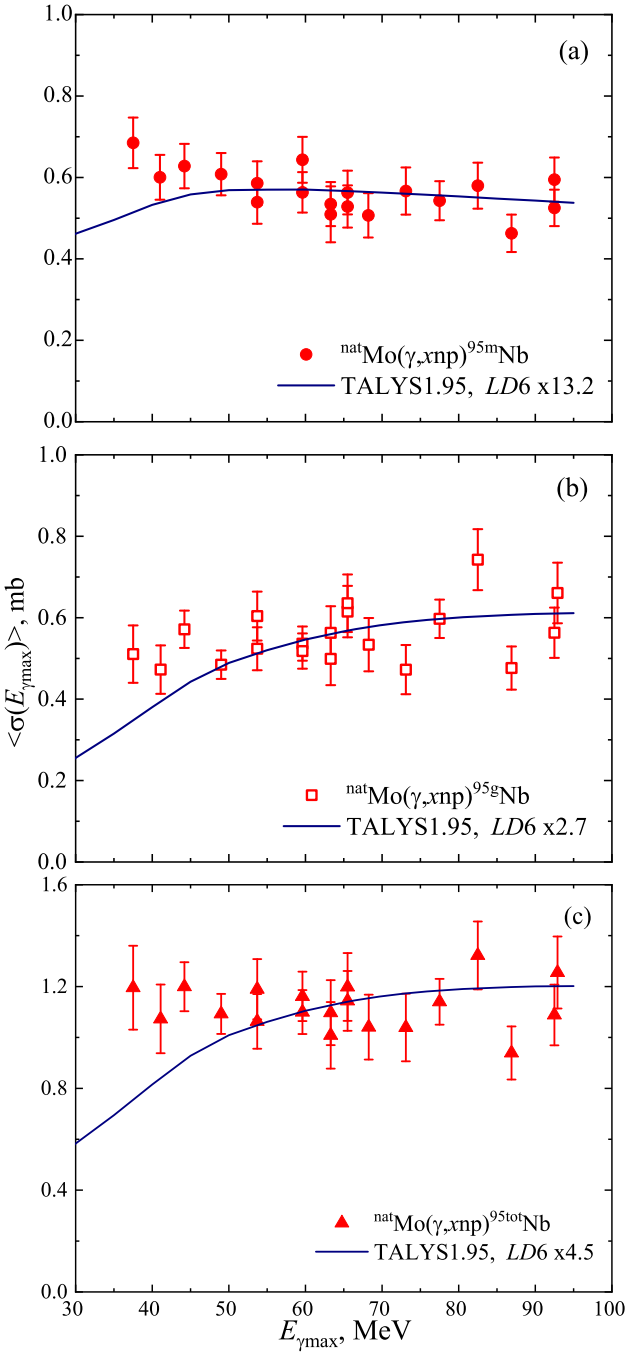

Fig. 8 Flux-averaged cross-sections $\langle\sigma(E_{\gamma\max})\rangle$ for the formation of ^{95m}Nb (**a**), ^{95g}Nb (**b**) on $^{\rm nat}$Mo, and total cross-section for the $^{\rm nat}$Mo$(\gamma, x{\rm np})^{95tot}$Nb reaction (**c**). Calculations were performed with the TALYS1.95 code for $LD6$

Table 1 Flux-averaged cross-sections for the ^{nat}Mo(γ, $x$np)^{95m,g,tot}Nb reactions

	$\langle\sigma(E_{\gamma max})\rangle$, mb		
$E_{\gamma max}$, MeV	Metastable	Ground	Total
37.50	0.68 ± 0.06	0.51 ± 0.07	1.19 ± 0.15
41.10	0.60 ± 0.06	0.47 ± 0.06	1.07 ± 0.13
44.20	0.63 ± 0.05	0.57 ± 0.05	1.20 ± 0.10
49.00	0.61 ± 0.05	0.48 ± 0.05	1.09 ± 0.11
53.70	0.54 ± 0.05	0.52 ± 0.05	1.06 ± 0.11
53.70	0.59 ± 0.05	0.60 ± 0.06	1.19 ± 0.12
59.60	0.56 ± 0.05	0.54 ± 0.05	1.10 ± 0.10
59.60	0.64 ± 0.06	0.52 ± 0.05	1.16 ± 0.10
63.30	0.53 ± 0.05	0.56 ± 0.07	1.09 ± 0.13
63.30	0.51 ± 0.07	0.50 ± 0.07	1.01 ± 0.14
65.50	0.53 ± 0.05	0.61 ± 0.06	1.14 ± 0.12
65.50	0.56 ± 0.05	0.64 ± 0.07	1.20 ± 0.13
68.25	0.51 ± 0.05	0.53 ± 0.07	1.04 ± 0.13
73.10	0.57 ± 0.06	0.47 ± 0.06	1.04 ± 0.13
77.50	0.54 ± 0.05	0.60 ± 0.05	1.14 ± 0.10
82.50	0.58 ± 0.06	0.74 ± 0.07	1.32 ± 0.13
86.90	0.46 ± 0.05	0.48 ± 0.05	0.94 ± 0.10
92.50	0.53 ± 0.04	0.56 ± 0.06	1.09 ± 0.12
92.90	0.59 ± 0.05	0.66 ± 0.07	1.25 ± 0.14

reaction were define on the assumption that the main channel in the formation of the ^{95m}Nb nucleus on natural molybdenum is the reaction on ^{96}Mo, the isotopic abundance of which is 16.68%. Accordingly, when assessing $\langle\sigma(E_{\gamma max})\rangle_Q$, we obtained our results taking into account this isotopic concentration in order to correctly compare measurement data from different laboratories. As can be seen from Fig. 9, our result $\langle\sigma(E_{\gamma max})\rangle_Q$ and the data of [41] are in reasonable agreement with each other.

It should be noted that according to the results of calculations of the normalized reaction yield $Y_i(E_{\gamma max})$, performed using cross-sections from the TALYS1.95 code (see Fig. 4), the statement about the dominant role of the ^{96}Mo(γ, p) reaction in the case of the formation of the ^{95m}Nb nucleus on natural Mo is valid at energies up to 30 MeV (provided the contribution of the dominant reaction is at least 90%).

5 Conclusions

In the present work, the experiment was performed on the beam of a linear electron accelerator LUE-40 RDC "Accelerator" NSC KIPT using the activation and off-line γ-ray spectrometric techniques. The bremsstrahlung flux-averaged cross-section $\langle\sigma(E_{\gamma max})\rangle_m$ of the ^{95m}Nb production in photonuclear reactions on natural Mo targets was determined for the first time. The bremsstrahlung end-point energy range was $E_{\gamma max}$ = 38–93 MeV.

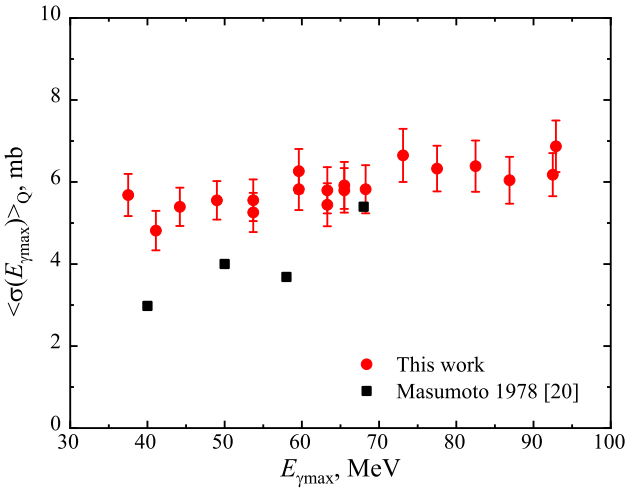

Fig. 9 Average cross-section per equivalent photon $\langle\sigma(E_{\gamma max})\rangle_Q$ for the ^{96}Mo(γ, p)^{95m}Nb reaction. The results of this work are denoted by red circles, black squares – from [41]. There is no information about experimental errors for data from [41]

Based on the experimental data on $\langle\sigma(E_{\gamma max})\rangle_m$ and the isomeric yield ratio IR, the values of $\langle\sigma(E_{\gamma max})\rangle_g$ and $\langle\sigma(E_{\gamma max})\rangle_{tot}$ for the formation of the ^{95}Nb nucleus in the ground state and for the total cross-section of the ^{nat}Mo(γ, $x$np) reaction were obtained in this work.

The calculation of the flux-averaged cross-sections $\langle\sigma(E_{\gamma max})\rangle$ was performed using the cross-sections $\sigma(E)$ for the studied reactions from the TALYS1.95 code for different level density models LD 1–6.

In the case of the ^{nat}Mo(γ, $x$np)^{95m}Nb reaction, the comparison showed a significant excess (about 13.2 times) of the experimental results over the theoretical flux-averaged cross-sections $\langle\sigma(E_{\gamma max})\rangle_m$. This result can be used to improve the TALYS code.

The calculation result with the level density model $LD6$ (microscopic level densities based on temperature-dependent Hartree-Fock-Bogoliubov calculations using the Gogny force from Hilaire's combinatorial tables) is the closest to the experimental cross-section data.

Acknowledgements The authors would like to thank the staff of the linear electron accelerator LUE-40 NSC KIPT, Kharkiv, Ukraine, for their cooperation in the realization of the experiment.

Funding Open access funding provided by The Ministry of Education, Science, Research and Sport of the Slovak Republic in cooperation with Centre for Scientific and Technical Information of the Slovak Republic

Data Availability Statement This manuscript has no associated data or the data will not be deposited. [Authors' comment: The authors declare that all data generated or analysed during this study are included in this published article.]

Declarations

Conflict of interest The authors declare that they have no known competing financial interests or personal relationships that could have appeared to influence the work reported in this paper.

References

1. IAEA, Handbook on photonuclear data for applications cross-sections and spectra, IAEA-TECDOC-1178, http://www-nds.iaea.org/publications/tecdocs/ (2000)
2. M.U. Khandaker, K. Kim, M.W. Lee et al., Nucl. Instrum. Methods **B269**, 1140 (2011). https://doi.org/10.1016/j.apradiso.2009.02.030
3. T.R. Allen, D.C. Crawford, Sci. Technol. Nucl. Install. **2007**, 97486 (2007). https://doi.org/10.1155/2007/97486
4. Accelerator driven systems: energy generation and transmutation of nuclear waste, Status report, IAEA, Vienna, IAEA-TECDO-985 (1997)
5. C.D. Bowman, Annu. Rev. Nucl. Part. Sci. **48**, 505 (1998). https://doi.org/10.1146/annurev.nucl.48.1.505
6. S.S. Dietrich, B.L. Berman, At. Data Nucl. Data Tables **38**, 199 (1988). https://doi.org/10.1016/0092-640X(88)90033-2
7. A.V. Varlamov, V.V. Varlamov, D.S. Rudenko, M.E. Stepanov, *INDC(NDS)-394* (IAEA NDS, Vienna, Austria, 1999)
8. E. Wolynec, A.R.V. Martinez, P. Gouffon et al., Phys. Rev. C **29**, 1137 (1984). https://doi.org/10.1103/PhysRevC.29.1137
9. E. Wolynec, M.N. Martins, Rev. Bras. Fis. **17**, 56 (1987)
10. V.V. Varlamov, B.S. Ishkhanov, V.N. Orlin, Phys. At. Nucl. **75**, 1339 (2012). https://doi.org/10.1134/S1063778812110191
11. V.V. Varlamov, B.S. Ishkhanov, V.N. Orlin, K.A. Stopani, Eur. Phys. J. A **50**, 114 (2014). https://doi.org/10.1140/epja/i2014-14114-x
12. V.V. Varlamov, A.I. Davydov, B.S. Ishkhanov, V.N. Orlin, Eur. Phys. J. A **54**, 74 (2018). https://doi.org/10.1140/epja/i2018-12508-4
13. V.V. Varlamov, A.I. Davydov, V.N. Orlin, Eur. Phys. J. A **57**, 287 (2021). https://doi.org/10.1140/epja/s10050-021-00594-6
14. V.V. Varlamov, A.I. Davydov, V. Kaidarova, V.N. Orlin, Phys. Rev. C **99**, 024608 (2019). https://doi.org/10.1103/PhysRevC.99.024608
15. M. Herman, R. Capote, B. V. Carlson, P. Oblozinsky, M. Sin, A. Trkov, H. Wienke, V. Zerkin, "EMPIRE: Nuclear reaction model code system for data evaluation," Nucl. Data Sheets **108**, 2655 (2007). EMPIRE - Nuclear Reaction Model Code // https://www-nds.iaea.org/empire/
16. A.J. Koning, S. Hilaire, and M.C. Duijvestijn, "TALYS-1.0," EPJ Web Conf., 211 (2008). Proc. Int. Conf. on Nuclear Data for Science and Technology, 22 - 27 Apr., 2007, Nice, France, (Eds.) O. Bersillon, F. Gunsing, E. Bauge, R. Jacqmin, and S. Leray. TALYS - based evaluated nuclear data library. http://www.TALYS.eu/home/
17. O. Iwamoto, N. Iwamoto, S. Kunieda, F. Minato, K. Shibata, The CCONE code system and its application to nuclear data evaluation for fission and other reactions. Nucl. Data Sheets **131**, 259 (2016)
18. T. Kawano, "CoH3: The coupled-channels and HauserFeshbach code," (2019). CNR2018: International Workshop on Compound Nucleus and Related Topics, LBNL, Berkeley, CA, USA, September 24–28, 2018, (Ed. J. Escher)
19. IAEA NDS database "Experimental Nuclear Reaction Data (EXFOR)", http://www-nds.iaea.org/exfor; USA NNDC database "CSISRS and EXFOR Nuclear Reaction Experimental Data", http://www.nndc.bnl.gov/exfor/exfor00.htm. Russia Lomonosov MSU Skobeltsyn INP CDFE database "Nuclear Reaction Database (EXFOR)", http://cdfe.sinp.msu.ru/exfor/index.php (2020)
20. Evaluated Nuclear Data File (ENDF), https://www.nndc.bnl.gov/endf/
21. R. Capote et al. RIPL-Reference Input Parameter Library for calculation of nuclear reactions and nuclear data evaluation. Nucl. Data Sheets **110**, 3107, (2009) https://www-nds.iaea.org/RIPL/
22. Data Center of Photonuclear Experiments, http://cdfe.sinp.msu.ru/
23. S.Y.F. Chu, L.P. Ekstrom, R.B. Firestone, The Lund/LBNL, Nuclear Data Search, Version 2.0, February 1999, WWW Table of Radioactive Isotopes, http://nucleardata.nuclear.lu.se/toi/
24. T. Kawano, Y.S. Cho, P. Dimitriou et al., Nucl. Data Sheets **163**, 109 (2020)
25. O.S. Deiev, I.S. Timchenko, S.M. Olejnik et al., Photonuclear reactions ^{nat}Ni(γ, xn)^{57}Ni and ^{nat}Ni(γ, xn)^{56}Ni in the energy range $E_{\gamma max}$ = 35–94 MeV // Nucl. Phys. A **1028**, 122542 (2022). https://doi.org/10.1016/j.nuclphysa.2022.122542
26. H. Naik, G. Kim, K. Kim et al., Nucl. Phys. A **948**, 28 (2016). https://doi.org/10.1016/j.nuclphysa.2016.01.015
27. S. Goriely, P. Dimitriou, M. Wiedeking et al., Eur. Phys. J. A **55**, 172 (2019). https://doi.org/10.1140/epja/i2019-12840-1. arXiv:1910.06966
28. H. Utsunomiya, I. Gheorghe, D.M. Filipescu et al., EPJ Web Conf. **239**, 01002 (2020). https://doi.org/10.1051/epjconf/202023901002
29. A.E. Avetisyan, R.V. Avetisyan, A.G. Barseghyan et al., Phys. At. Nucl. **84**, 245 (2021). https://doi.org/10.1134/S1063778821020034
30. O.S. Deiev, I.S. Timchenko, S.M. Olejnik, V.A. Kushnir, V.V. Mytrochenko, S.A. Perezhogin, Cross-sections of photoneutron reactions on ^{181}Ta at $E_{\gamma max}$ up to 95 MeV. Phys. Rev. C **106**, 024617 (2022). https://doi.org/10.1103/PhysRevC.106.024617
31. I.S. Timchenko, O.S. Deiev, S.N. Olejnik, S.M. Potin, L.P. Korda, V.A. Kushnir, V.V. Mytrochenko, S.A. Perezhogin, A. Herzáň, Production of ^{180m}Hf in photoproton reaction ^{181}Ta(γ, p) at energy $E_{\gamma max}$ = 35–95 MeV Eur. Phys. J. **A59** 268 (2023), https://doi.org/10.1140/epja/s10050-023-01186-2; arXiv:2308.10339
32. I.S. Timchenko, O.S. Deiev, S.M. Olejnik, S.M. Potin, V.A. Kushnir, V.V. Mytrochenko, S.A. Perezhogin, V.A. Bocharov, Isomeric pair ^{95m,g}Nb in the photonuclear reactions on ^{nat}Mo at the bremsstrahlung end-point energy of 38–93 MeV // Chinese Phys. **C47**, (2023) 124002, https://doi.org/10.1088/1674-1137/acfaed, arXiv:2308.02243
33. A.N. Vodin, O.S. Deiev, I.S. Timchenko, S.N. Olejnik, Cross-sections for the ^{27}Al(γ, x)^{24}Na multi-particle reaction at $E_{\gamma max}$ = 35–95 MeV. Eur. Phys. J. **A57**, 207 (2021). https://doi.org/10.1140/epja/s10050-021-00483-y. arXiv:2012.14475
34. J.N. Orce, At. Data Nucl. Data Tables **146**, 101511 (2022). arXiv:2110.00979
35. B.S. Ishkhanov, I.M. Kapitonov, A.A. Kuznetsov, V.N. Orlin, H.D. Yoon, Photonuclear reactions on molybdenum isotopes. Phys. At. Nucl. **77**, 1362 (2014). https://doi.org/10.1134/S106377881410007X. (**Yadernaya Fizika 77 (2014) 1427**)

36. B.S. Ishkhanov, I.M. Kapitonov, A.A. Kuznetsov et al., Photodisintegration of molybdenum isotopes. Moscow Univ. Phys. Bull. **1**, 35 (2014)
37. O.S. Deiev, I.S. Timchenko, S.N. Olejnik et al., Cross-sections for the ^{27}Al$(\gamma, x)^{22}$Na multichannel reaction with the 28.3 MeV difference of the reaction thresholds. Chin. Phys. C **46**, 064002 (2022). https://doi.org/10.1088/1674-1137/ac5733. arXiv:2105.12658
38. O.S. Deiev, I.S. Timchenko, S.N. Olejnik et al., Photonuclear reactions ^{65}Cu$(\gamma, n)^{64}$Cu and ^{63}Cu$(\gamma, xn)^{63-x}$Cu cross-sections in the energy range $E_{\gamma max}$ = 35–94 MeV. Chin. Phys. C **46**, 124001 (2022). https://doi.org/10.1088/1674-1137/ac878a
39. K.S. Kim, M.DSh. Rahman, M. Lee, G. Kim et al., Measurement of isomeric yield ratios for ^{93}Nb$(\gamma, 4n)^{89m,g}$Nb and ^{nat}Mo$(\gamma, xnp)^{95m,g}$Nb reactions with 50-, 60-, and 70-MeV bremsstrahlung. J. Radioanal. Nucl. Chem. **287**, 869 (2011). https://doi.org/10.1007/s10967-010-0839-3
40. H. Naik, G. Kim, K. Kim, M. Zaman et al., Independent isomeric yield ratios of ^{95m,g}Nb in the ^{nat}Mo(γ, xnp) and ^{nat}Zr(p, xn) reactions. J. Radioanal. Nucl. Chem. **300**, 1121 (2014). https://doi.org/10.1007/s10967-014-3045-x
41. K. Masumoto, T. Kato, N. Suzuki, Activation yield curves of photonuclear reactions for multielement photon activation analysis. Nucl. Instrum. Meth. **157**, 567 (1978)
42. H. Matsumura, K. Washiyama, H. Haba et al., Radiochim. Acta **88**, 313 (2000)
43. V. Di Napoli, A.M. Lacerenza, F. Salvetti et al., Lett. Nuovo Cim. **1**, 835 (1971)
44. T. Kato, O. Yoshinaga, *Yields of Photonuclear Reactions for Photon-Activation Analysis with High Energy Bremsstrahlung*, vol. 19 (Talanta Pergamon Press, 1972), p.515
45. T. Kato, Quantitative evaluation of the photon-activation analysis. J. Radioanal. Chem. **16**, 307 (1973)
46. S.R. Palvanov, O. Razhabov, Isomeric yield ratios of photonuclear reactions at $E_{\gamma max}$ 25 and 30 MeV. At. Energy **87**, 533 (1999)
47. T.D. Thiep, T.T. An, N.T. Khai et al., The isomeric ratios in some photonuclear reactions (γ, n), (γ, p), $(\gamma,2n)$ and (γ, np) induced by bremsstrahlung with end-point energies in the giant dipole resonance region. Phys. Part. Nucl. Lett. **6**, 126 (2009). https://doi.org/10.1134/S1547477109020058
48. T.D. Thiep, T.T. An, P.V. Cuong et al., Isomeric ratios in photonuclear reactions of molybdenum isotopes induced by bremsstrahlung in the giant dipole resonance region. Phys. Part. Nucl. Lett. **14**, 102 (2017). https://doi.org/10.1134/S1547477117010241
49. K.S. Kim, M.DSh. Rahman, M. Lee, G. Kim et al., Measurement of isomeric yield ratios for ^{93}Nb$(\gamma, 4n)^{89m,g}$Nb and ^{nat}Mo$(\gamma, xnp)^{95m,g}$Nb reactions with 50-, 60-, and 70-MeV bremsstrahlung. J. Radioanal. Nucl. Chem. **287**, 869 (2011). https://doi.org/10.1007/s10967-010-0839-3
50. H. Naik, G. Kim, K. Kim, M. Zaman et al., Independent isomeric yield ratios of ^{95m,g}Nb in the ^{nat}Mo(γ, xnp) and ^{nat}Zr(p, xn) reactions. J. Radioanal. Nucl. Chem. **300**, 1121 (2014). https://doi.org/10.1007/s10967-014-3045-x
51. N. Mutsuro, Y. Ohnuki, K. Sato, M. Kimura, Photoneutron cross-sections for Ag^{107}, Mo^{92} and Zr^{90}. J. Phys. Soc. Jpn. **14**, 1649 (1959). https://doi.org/10.1143/JPSJ.14.1649
52. H. Beil, R. Bergire, P. Carlos, A. Lepretre et al., A study of the photoneutron contribution to the giant dipole resonance in doubly even Mo isotopes. Nucl. Phys. A **227**, 427 (1974). https://doi.org/10.1016/0375-9474(74)90769-6
53. A.N. Dovbnya, M.I. Aizatsky, V.N. Boriskin et al., Beam parameters of an S-band electron linac with beam energy of 30–100 MeV. Probl. At. Sci. Technol. **2**, 11 (2006)
54. M.I. Aizatskyi, V.I. Beloglazov, V.N. Boriskin et al., State and prospects of the linac of nuclear-physics complex with energy of electrons up to 100 MeV. Probl. At. Sci. Technol. **3**, 60 (2014)
55. V.V. Mytrochenko, L.I. Selivanov, VPh. Zhyglo et al., Magnetic system for cleaning the gamma beam at the LUE-40 linac output. Probl. Atom. Scien. Technol. **3**, 62 (2022). https://doi.org/10.46813/2022-139-062
56. O.S. Deiev, I.S. Timchenko, S.M. Olejnik et al., Photonuclear reactions cross-section at energies up to 100 MeV for different experimental setups. Probl. At. Sci. Technol. **5**, 11 (2022). https://doi.org/10.46813/2022-141-011
57. S. Agostinelli et al., Electron and positron incident. Methods Phys. **A506**, 250, (2003) http://GEANT4.9.2.web.cern.ch/GEANT4.9.2/
58. O.S. Deiev, I.S. Timchenko, S.N. Olejnik, V.A. Kushnir, V.V. Mytrochenko, S.A. Perezhogin, Isomeric ratio of the ^{181}Ta$(\gamma, 3n)^{178m,g}$Ta reaction products at energy $E_{\gamma max}$ up to 95 MeV. Chin. Phys. C **46**, 014001 (2022). https://doi.org/10.1088/1674-1137/ac2a95
59. A.N. Vodin, O.S. Deiev, I.S. Timchenko, S.N. Olejnik, N.I. Ayzatsky, V.A. Kushnir, V.V. Mytrochenko, S.A. Perezhogin, Photoneutron cross-sections for the reactions ^{181} Ta$(\gamma, xn; x = 1 - 8)^{181-x}$Ta at $E_{\gamma max}$ = 80–95 MeV. Eur. Phys. J. **A57**, 208 (2021). https://doi.org/10.1140/epja/s10050-021-00484-x. arXiv:2103.09859
60. A.N. Vodin, O.S. Deiev, VYu. Korda et al., Photoneutron reactions on ^{95}Nb at $E_{\gamma max}$ = 33–93 MeV. Nucl. Phys. A **1014**, 122248 (2021). https://doi.org/10.1016/j.nuclphysa.2021.122248. arXiv:2101.08614
61. A. Gilbert, A.G.W. Cameron, A composite nuclear-level density formula with shell corrections. Can. J. Phys. **43**, 1446 (1965). https://doi.org/10.1139/p65-139
62. W. Dilg, W. Schantl, H. Vonach, M. Uhl, Level density parameters for the back-shifted fermi gas model in the mass range $40<A<250$. Nucl. Phys. A **217**, 269 (1973). https://doi.org/10.1016/0375-9474(73)90196-6
63. A.V. Ignatyuk, K.K. Istekov, G.N. Smirenkin, Role of collective effects in the systematics of nuclear level densities. Sov. J. Nucl. Phys. **29**, 450 (1979)
64. A.V. Ignatyuk, J.L. Weil, S. Raman, S. Kahane, Density of discrete levels in ^{116}Sn. Phys. Rev. C **47**, 1504 (1993). https://doi.org/10.1103/PhysRevC.47.1504
65. S. Goriely, F. Tondeur, J.M. Pearson, A Hartree-Fock nuclear mass table. At. Data Nucl. Data Tables **77**, 311 (2001). https://doi.org/10.1006/adnd.2000.0857
66. S. Goriely, S. Hilaire, A.J. Koning, Improved microscopic nuclear level densities within the Hartree-Fock-Bogoliubov plus combinatorial method. Phys. Rev. C **78**, 064307 (2008). https://doi.org/10.1103/PhysRevC.78.064307
67. S. Hilaire, M. Girod, S. Goriely, A.J. Koning, Temperature-dependent combinatorial level densities with the D1M Gogny force. Phys. Rev. C **86**, 064317 (2012). https://doi.org/10.1103/PhysRevC.86.064317
68. A.N. Vodin, O.S. Deiev, I.S. Timchenko, S.M. Olejnik, V.A. Kushnir, V.V. Mytrochenko, S.O. Perezhogin, V.O. Bocharov, Cross-sections of photonuclear reactions on ^{nat}Mo targets at end-point bremsstrahlung energy up to $E_{\gamma max}$ = 100 MeV. Probl. At. Sci. Technol. **3**, 98 (2021). https://doi.org/10.46813/2021-133-098